

# Low-energy excitations in the $S = \frac{1}{2}$ molecular nanomagnet $\text{K}_6[\text{V}_{15}^{\text{IV}}\text{As}_6\text{O}_{42}(\text{H}_2\text{O})] \cdot 8\text{H}_2\text{O}$ from proton NMR and $\mu\text{SR}$

D. Prociassi,<sup>1,\*</sup> A. Lascialfari,<sup>2,3,†</sup> E. Micotti,<sup>3</sup> M. Bertassi,<sup>3</sup> P. Carretta,<sup>3</sup> Y. Furukawa,<sup>4</sup> and P. Kögerler<sup>1</sup>

<sup>1</sup>*Department of Physics and Astronomy, and Ames Laboratory, Iowa State University, Ames, Iowa 50011, USA*

<sup>2</sup>*Istituto di Fisiologia Generale e Chimica Biologica, Università di Milano, I-20134 Milano, Italy*

<sup>3</sup>*CNR-INFM and Dipartimento di Fisica “A. Volta,” Università di Pavia, I-27100 Pavia, Italy*

<sup>4</sup>*Division of Physics, Graduate School of Sciences, Hokkaido University, Sapporo 060-0810, Japan*

(Received 22 March 2006; published 15 May 2006)

Zero- and longitudinal-field muon-spin-rotation ( $\mu\text{SR}$ ) and  $^1\text{H}$  NMR measurements on the  $S = \frac{1}{2}$  molecular nanomagnet  $\text{K}_6[\text{V}_{15}^{\text{IV}}\text{As}_6\text{O}_{42}(\text{H}_2\text{O})] \cdot 8\text{H}_2\text{O}$  are presented. In LF experiments, the muon asymmetry  $P(t)$  was fitted by the sum of three different exponential components with fixed weights. The different muon relaxation rates  $\lambda_i$  ( $i=1,2,3$ ) and the low-field  $H=0.23$  T  $^1\text{H}$  NMR spin-lattice relaxation rate  $1/T_1$  show a similar behavior for  $T > 50$  K: starting from room temperature they increase as the temperature is decreased. The increase of  $\lambda_i$  and  $1/T_1$  can be attributed to the “condensation” of the system toward the lowest-lying energy levels. The gap  $\Delta \sim 550$  K between the first and second  $S = \frac{3}{2}$  excited states was determined experimentally. For  $T < 2$  K, the muon relaxation rates  $\lambda_i$  stay constant, independently of the field value  $H \leq 0.15$  T. The behavior for  $T < 2$  K strongly suggests that, at low  $T$ , the spin fluctuations are not thermally driven but rather originate from quasielastic intramolecular or intermolecular magnetic interactions. We suggest that the very-low-temperature relaxation rates could be driven by energy exchanges between two almost degenerate  $S = \frac{1}{2}$  ground states and/or by quantum effects.

DOI: 10.1103/PhysRevB.73.184417

PACS number(s): 75.45.+j, 76.60.-k, 76.75.+i

## I. INTRODUCTION

The magnetic properties of molecular nanomagnets have attracted considerable interest for their implications in fundamental physics and possible applications like magnetic storage, magnetoelectronics, and quantum computing.<sup>1,2</sup> These clusters are formed by identical mesoscopic magnetic entities, each one isolated from the others by a hydrophobic organic screen. Therefore the molecules act as individual quantum nanomagnets [single-molecule magnet (SMM)], enabling one to probe the crossover between quantum and classical physics at low temperature. The fundamental properties, such as, e.g., the ground-state spin, the magnetic anisotropy, and intramolecular and intermolecular interactions, can be determined accurately. Some of the newest and most striking phenomena observed at very low temperatures are the magnetic bistability, the quantum tunneling of the magnetization, quantum phase interference (Berry phase), quantum coherence, etc.<sup>2-6</sup> Recently, the possibility of using low-spin systems for quantum computation was addressed by the synthesis of compounds with small dipolar interactions (a factor  $10^{-3}$  lower than the high-spin systems) that allow one to keep quantum coherence. Together with the most famous Mn(12) (Refs. 1 and 2) and Fe(8) (Refs. 1 and 7) SMM's, the polyoxovanadate compounds were extensively studied.<sup>1,8-14</sup>

Among them, the molecule  $\text{K}_6[\text{V}_{15}^{\text{IV}}\text{As}_6\text{O}_{42}(\text{H}_2\text{O})] \cdot 8\text{H}_2\text{O}$  [in short, V(15)] constitutes an example of a low-spin system. This molecular complex forms a lattice which contains two molecules per cell. Its ground state presents two Kramers doublets with total spin  $S = \frac{1}{2}$ , the doublets being split, in zero field, by  $\sim 0.08$  K. This spin value is given by the arrangement of 15 V(IV)  $s = \frac{1}{2}$  ions in three layers, two hexagons with total spin  $S_h = 0$  sandwiching a triangle with  $S_t = \frac{1}{2}$ .<sup>8-14</sup> The origin of the ground-state splitting resides pos-

sibly in intramolecular, hyperfine, and Dzyaloshinski-Moriya interactions. The values of intermolecular interactions were estimated to be  $\theta \sim 10$  mK, obtained from the susceptibility behavior in the region where it follows a Curie-Weiss law  $\chi = C/(T + \theta)$  ( $C \sim 0.7 \mu_B$  K/T).<sup>13</sup> Thus, the exchange intramolecular interactions between V(IV) ions are dominant [Fig. 1(a)]: the main antiferromagnetic (AF) exchange interaction  $J \sim 800$  K couples three pairs of spins inside the hexagons, while the remaining AF ones are inside the hexagon ( $J' \sim 150$  K and  $J'' \sim 300$  K) and between the hexagon and the triangle ( $J_1 \sim 150$  K and  $J_2 \sim 300$  K).<sup>8-12</sup> The AF exchange interaction between the spins in the triangle is very weak ( $J_0 \sim 2.5$  K). With these interaction schemes, the first  $S = \frac{3}{2}$  excited state lies 3.8 K above the  $S = \frac{1}{2}$  ground-state doublet. The successive excited ( $S = \frac{3}{2}$ ) state lies some hundredths of K above the ground state<sup>8</sup> [Fig. 1(b)]. The lowest-lying levels structure was confirmed by magnetization  $M(H)$  and neutron scattering measurements, and new quantum effects were discovered.<sup>13,14</sup> Particularly, for the sake of completeness it should be remarked that for constant  $T < 0.5$  K, at thermal equilibrium,  $M(H)$  clearly exhibits a step at a critical field  $H_c \sim 2.8$  T, where the  $S = \frac{1}{2}$  ground state changes to  $S = \frac{3}{2}$  (Ref. 9) (level crossing). On the other hand, nonequilibrium magnetization measurements with high-field sweeping rates revealed a “butterfly” hysteresis loop around zero magnetic field.<sup>9</sup> These effects have been associated with phonon bottleneck and Dzyaloshinski-Moriya interaction.<sup>9,13,14</sup>

At variance with the possibilities of macroscopic techniques, NMR and muon-spin-rotation ( $\mu\text{SR}$ ) use local probes to determine the microscopic behavior of local spins. With the aim of studying the local spin dynamics of  $\text{V}^{4+}$  spins as a function of temperature ( $0.3 < T < 300$  K) at constant fields and as a function of field at constant low  $T$ , we

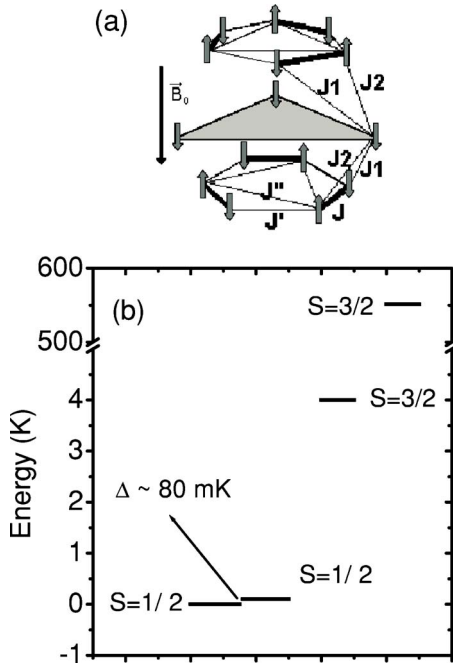


FIG. 1. (Color online) (a) Schematic view of the low-spin cluster  $K_6[V_{15}^{IV}As_6O_{42}(H_2O)] \cdot 8H_2O$ , with the different exchange coupling constants  $B_0$  being the external magnetic field. Best fitting values of the exchange constants obtained from susceptibility data (Refs. 8, 13, and 14) are reported in the text. (b) Scheme of the lowest-lying energy levels of V(15) ( $S$ =total spin). The highest  $S=3/2$  is almost degenerate with another  $S=3/2$  level (Ref. 8).

performed  $\mu$ SR (in zero-field and longitudinal applied magnetic fields) and proton NMR experiments, with particular attention to the temperature behavior of the muon longitudinal and nuclear spin-lattice relaxation rates.

## II. EXPERIMENTAL DETAILS

Microcrystalline samples of  $K_6[V_{15}^{IV}As_6O_{42}(H_2O)] \cdot 8H_2O$  were prepared as described in Ref. 8. In order to characterize the magnetic properties of the sample, we performed magnetization measurements using a MPMS-XL7 Quantum Design magnetometer, in the temperature range 1.8–300 K at different constant magnetic fields  $H=0.05, 0.15, 0.23,$  and  $2.7$  T, corresponding to the fields used in  $\mu$ SR and NMR measurements.

The  $\mu^+$ SR data were collected at the ISIS facility, Rutherford Appleton Laboratory (UK), in the temperature range 0.3–300 K, in zero field and longitudinal magnetic fields (LF)  $H=0.05$  and  $0.15$  T. Data at constant  $T=0.34$  and  $3.8$  K were also collected, in the LF range  $0.05 \leq H \leq 0.3$  T. In LF- $\mu$ SR experiments, the measured muon asymmetry  $P(t)$  shows that the muon spin relaxes at any temperature and can be fitted using a sum of three different exponential components. This means that the muons implant in, at least, three different sites. By taking into account that the total asymmetry was  $\sim 24$ , after the usual background subtraction the function used to fit the data was

$$P(t) = a_1 \exp(-\lambda_1 t) + a_2 \exp(-\lambda_2 t) + a_3 \exp(-\lambda_3 t), \quad (1)$$

where  $\lambda_1, \lambda_2,$  and  $\lambda_3$  are muon longitudinal relaxation rates ( $\lambda_1 > \lambda_2 > \lambda_3$ ) and  $a_1 \sim 25\%, a_2 \sim 50\%,$  and  $a_3 \sim 25\%$  their

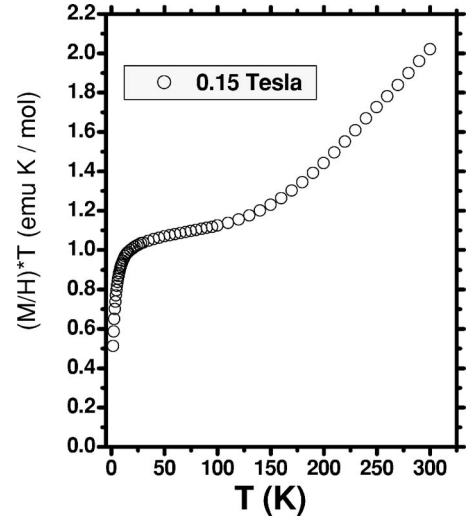


FIG. 2.  $(M/H) \times T$  vs temperature at applied magnetic field  $H = 0.15$  T. The data were taken in V(15) powders, in field-cooling conditions.

relative weights, kept constant over the whole investigated temperature range.

$^1H$ -NMR measurements were performed by a pulsed Fourier-transform spectrometer for magnetic fields  $H=0.23$  and  $2.7$  T in the temperature range 1.5–300 K. The nuclear spin-lattice relaxation time  $T_1$  was measured by the saturation method at the peak position in the  $^1H$ -NMR spectrum.<sup>15</sup> The nuclear magnetization recovery deviates from a single-exponential behavior, as already reported by ProciSSI *et al.*,<sup>16</sup> and also in different molecular magnets such as Fe(6),<sup>17</sup> Fe(8),<sup>18</sup> and Fe(10).<sup>19</sup>  $T_1$  “average” values were determined by the initial slope of the recovery curve as in the case of other molecular magnets.<sup>16</sup>

## III. RESULTS AND DISCUSSION

The results  $(M/H) \times T$  for  $H=0.15$  T vs temperature are reported in Fig. 2. It is noted that the qualitative behavior of the measured susceptibility is the same as the one reported previously<sup>8</sup> and that the variation in the quantity  $(M/H) \times T$  with increasing field is small (data not reported). The current experimental results confirm the already known scheme and values of the exchange constants. The different  $\mu$ SR and NMR relaxation rates (RR’s) for  $T > 50$  K show qualitatively the same temperature behavior at  $H \leq 0.23$  T [see Figs. 3(a) and 4]: starting from room temperature they increase as the temperature is decreased down to  $T \sim 50(10)$  K. In the intermediate-temperature region  $4 < T < 50$  K,  $\mu$ SR data follow the  $(M/H) \times T$  behavior while proton NMR  $1/T_1$  slightly increases on decreasing  $T$ . For  $T < 2$  K the muon relaxation rates stay constant within the experimental error and their value is almost independent of magnetic field. This is further confirmed by measurements at constant temperatures. At  $T=0.34$  and  $3.8$  K, the muon relaxation rates  $\lambda_i$  stay constant for  $0.05 \leq H \leq 0.2$  T [Fig. 3(b)]. At  $T=0.34$  K,  $\lambda_1$  and  $\lambda_2$  have a slight decrease for fields  $H > 0.2$  T (data not reported). For  $H=2.7$  T,  $^1H$  NMR

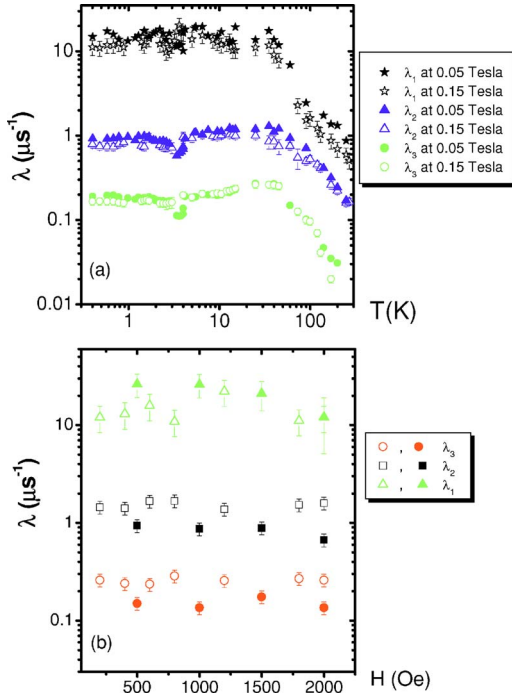


FIG. 3. (Color online) (a) Muon longitudinal relaxation rates (MLRR's) corresponding to three different muon implantation sites on V(15) powders, obtained from fit of the polarization (see text). The magnetic fields were applied in the longitudinal direction. The relaxation rate  $\lambda_1$  has a big experimental error due to uncertainty in short times fits. (b) MLRR as a function of longitudinal applied field at two constant temperatures (solid symbols,  $T=0.34$  K; open symbols,  $T=3.8$  K).

$1/T_1$  for  $T > 50$  K shows a behavior similar to low-field data while it decreases for lower temperatures. These high-field data are not the focus of the current work, and for an appropriate discussion we refer to Ref. 15.

For the analysis of the  $H \leq 0.23$  T relaxation rate data in the range  $T > 50$  K, we used a semiclassical model. Starting from general arguments,<sup>20,21</sup> in a weak-collision approach  $\lambda_i$  ( $1/T_1$ ) is proportional to the spectral density of the (single-ion) electronic spin fluctuations. It can be proved that in SMM  $\lambda_i$  ( $1/T_1$ ) can be expressed as<sup>22–26</sup>

$$\lambda_i \left( \frac{1}{T_1} \right) \propto J_{S_z S_z}(\omega_L), \quad (2)$$

where  $z$  is the direction of the applied magnetic field,  $S_z$  the  $z$  component of the total spin and  $J_{S_z S_z}(\omega_L)$  [in short  $J(\omega_L)$ ] the spectral density obtained as Fourier transform of the spin-spin correlation function  $G(t)$ . In Eq. (2), with respect to usual expression for  $\lambda_i$  ( $1/T_1$ ),<sup>20,21</sup> the single-ion spin  $s_z$  is substituted by the total spin  $S_z$ .

By hypothesizing an exponential decay for  $G(t)$ , Eq. (2) in molecular AF rings was very recently<sup>23</sup> suggested to reduce to (see also Ref. 24)

$$\frac{1}{T_1 \chi T} = A \frac{\Gamma_0(T)}{\Gamma_0^2(T) + \omega_L^2}, \quad (3)$$

where  $\Gamma_0$  is a frequency whose inverse  $\tau_0$  represents the average lifetime broadening of different discrete energy sublev-

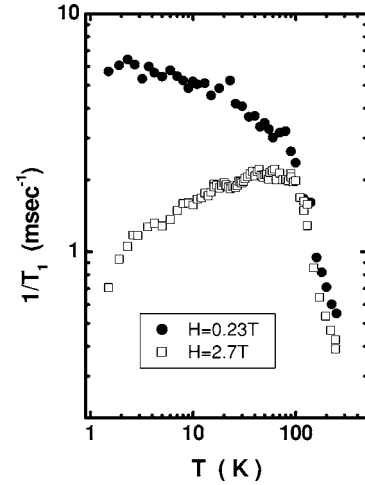


FIG. 4.  $^1\text{H}$  NMR spin-lattice relaxation rates in V(15) powders, at two different applied magnetic fields corresponding to frequencies 9.79 MHz (0.23 T) and 114.96 MHz (2.7 T).

els, thermally populated. Furthermore, we notice that in the temperature range here considered, V(15) can be considered a two-level system, the two energy levels being the first  $S=\frac{3}{2}$  excited state [ $E_2^{\frac{3}{2}}(\text{I})=3.8$  K] and the second  $S=\frac{3}{2}$  excited state [ $E_2^{\frac{3}{2}}(\text{II}) \sim$  some hundredths of K]. As a consequence, in Eq. (3),  $\Gamma_0$  represents the inverse lifetime of the lowest-energy level  $E_2^{\frac{3}{2}}(\text{I})$ , linked to the inverse lifetime  $\Gamma_1$  of  $E_2^{\frac{3}{2}}(\text{II})$  by the detailed balance equation<sup>27–29</sup>

$$\Gamma_0 = \Gamma_1 e^{-\Delta/k_B T}, \quad (4)$$

where  $\Delta = E_2^{\frac{3}{2}}(\text{I}) - E_2^{\frac{3}{2}}(\text{II})$ . The behavior of  $\Gamma_0(T)$  is possibly related to the temperature dependence of the spin-phonon interaction and to other terms related to dipolar and hyperfine intermolecular and intramolecular interactions. Equation (3) shows that the nuclear relaxation is driven by a single characteristic time  $\tau_0$ . Taking into account that the lifetime broadening is limited by the intermolecular interaction  $\Theta \sim 10$  mK, to fit the experimental data we finally assumed the expression

$$\Gamma_0 = B + \Gamma_1 e^{-\Delta/k_B T}, \quad (5)$$

where  $B=0.21 \times 10^9$  rad Hz is the intermolecular interaction frequency.

In this way the free parameters for fitting experimental data are  $\Gamma_1$  and  $\Delta$ , while  $A$  works as a rescaling factor and the  $\chi T$  values used in Eq. (3) are the experimental ones extracted from superconducting quantum interference device (SQUID) data. The energy gap  $\Delta$  between the two levels was determined by fitting the experimental  $\Gamma_0$  vs  $k_B T/\Delta$  NMR and  $\mu\text{SR}$  data, Fig. 5, in the range  $k_B T/\Delta > 0.1$ ; we obtained  $\Delta=551(43)$  K and  $\Gamma_1 = \Gamma_1^{\text{NMR}} = \Gamma_1^{\mu\text{SR}} = 0.226(0.028) \times 10^{11}$  rad Hz. By using these values in expression (5), with the formula (3) we fitted NMR data at  $H=0.23$  T and  $\mu\text{SR}$   $\lambda_2$  data at  $H=0.05$  and 0.15 T, obtaining  $A^{\text{NMR}}=8.5(1) \times 10^{17}$   $\text{rad}^2 \text{ Hz}^2/\text{K}$  and  $A^{\mu\text{SR}}(\lambda_2)=2.4(1) \times 10^{17}$   $\text{rad}^2 \text{ Hz}^2/\text{K}$ . It should be noted that  $\Delta$  and  $\Gamma_0$  are the same for NMR and  $\mu\text{SR}$  data. The fitting curves are reported in Fig. 6(a) ( $\mu\text{SR}$ )

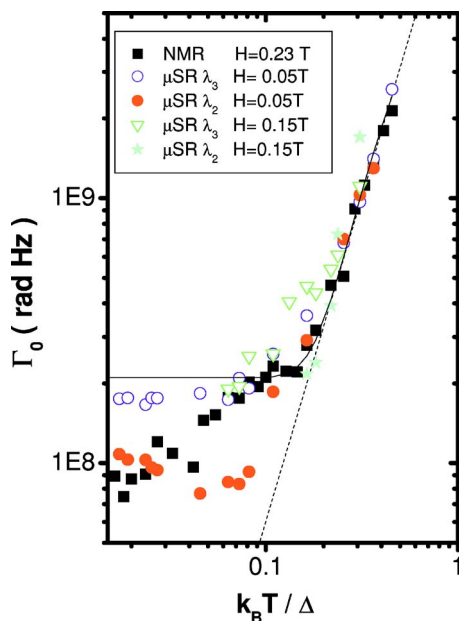


FIG. 5. (Color online) Inverse lifetime  $\Gamma_0$  as a function of  $k_B T / \Delta$  extracted from different NMR and  $\mu$ SR experimental data, with proper rescaling factor  $A$  [see Eq. (3)]. The solid line represents the law  $\Gamma_0 = B + \Gamma_1 e^{-\Delta/k_B T}$ , with  $\Delta = 551$  K and  $\Gamma_1 = 0.226 \times 10^{11}$  rad Hz, while the dashed line traces the law  $\Gamma_0 = k T^{2.45}$  ( $k = 1.7 \times 10^{10}$ ).

and Fig. 6(b) (NMR). We chose  $\lambda_2$  because statistically it is more significant as the muons stopping in the related site have the biggest relative weight in the total muon polarization.

We would like to remark that with our set of  $T > 50$  K experimental data we were able to determine experimentally an estimate of the energy of the second excited  $S = \frac{3}{2}$  level.

Noticeably it should be also remarked that  $\Gamma(T)$  data for  $T > 50$  K could be fitted as well with a power law of the form  $\Gamma_0 = k T^{2.45}$  (fitting value  $k = 1.7 \times 10^{10}$ ), in agreement with results on AF rings,<sup>23</sup> grids,<sup>25</sup> and high-spin clusters.<sup>26</sup> So the exponential behavior and power law are indistinguishable in the temperature range chosen (see also Fig. 5). The existence of a single characteristic time  $1/\Gamma_0$  that allows one to fit experimental data was recently confirmed by theoretical calculations starting from first principles.<sup>24</sup> In Ref. 24, the characteristic time has an exponential behavior.

In the intermediate temperature region,  $4 < T < 50$  K, the two-level scheme is no longer applicable, as the fine structure of the lowest-lying levels starts to become important. For this reason our model cannot be applied in this temperature region even though the  $\mu$ SR data qualitatively follow the theoretical fits, Eq. (4).

Let us now briefly comment on the  $\mu$ SR relaxation rates for  $T < 2$  K that stay constant independently of the muon implantation site and the applied magnetic field. This behavior indicates that, in this temperature region, the muon relaxation is possibly driven by quantum effects coming from frustration effects, with spin fluctuations whose frequencies do not depend on temperature and field. A second possibility is that  $\lambda_i$  are driven by fluctuations of the total magnetization between the two lowest-lying  $S = \frac{1}{2}$  doublets, whose energy

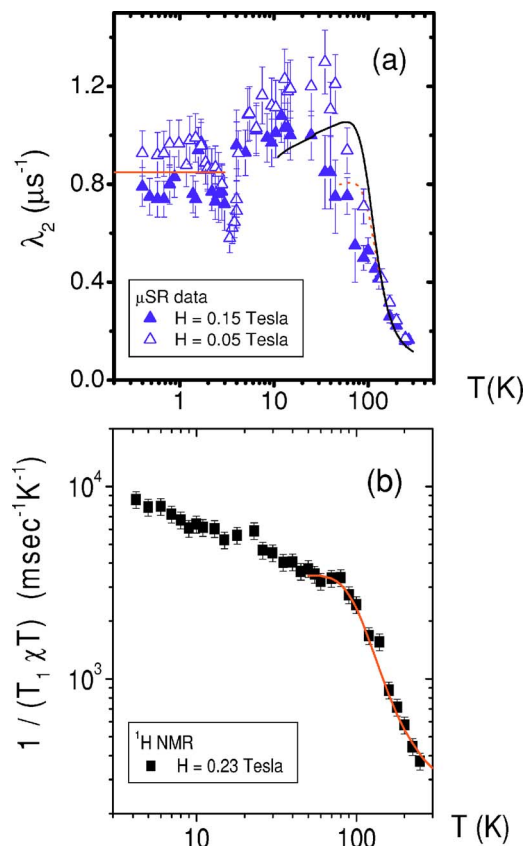


FIG. 6. (Color online) (a) Fits of the (intermediate) muon longitudinal relaxation rate  $\lambda_2$  for two different longitudinal magnetic fields (solid line,  $H = 0.05$  T; dashed line,  $H = 0.15$  T) by means of the semiclassical model reported in the text. At low temperatures  $T < 2$  K,  $\lambda_2$  reaches a plateau. (b) Fit (solid line) of the  $H = 0.23$  T spin-lattice relaxation rate  $^1\text{H}$  NMR data as a function of temperature by means of the same model used for  $\mu$ SR data.

difference is 0.08 K. The current set of experimental data is not sufficient to distinguish between the two hypotheses.

In summary, in the low-spin system V(15), we determined experimentally the position of the second  $S = \frac{3}{2}$  excited level by measuring, in the range  $50 < T < 300$  K, the muon longitudinal relaxation rate  $\lambda$  and the proton NMR spin-lattice relaxation rate. For  $0.3 < T < 2$  K, the  $\mu$ SR longitudinal relaxation rates  $\lambda_i$  are independent of field ( $H \leq 0.15$  T) and temperature, thus suggesting quantum effects on the muon relaxation. The spin fluctuations that drive the muon relaxation can originate from the two  $S = \frac{1}{2}$  ground-state doublets or from spin frustration.

#### ACKNOWLEDGMENTS

F. Pratt is gratefully acknowledged for help in the experimental  $\mu$ SR measurements. One of the authors (Y.P.) thanks the 21 Century COE Programs “Topological Science and Technology” at Hokkaido University and the Sumitomo Foundation for financial support. This work was supported by FIRB project RBNE01YLKN-2001, RTB Quemolna, and NoE MAGMANET.

- \*Present address: Brain Imaging Center, California Institute of Technology, Pasadena, CA 91125, USA.
- †Electronic address: lascialfari@fisicavolta.unipv.it
- <sup>1</sup>D. Gatteschi, A. Caneschi, L. Pardi, and R. Sessoli, *Science* **265**, 54 (1994).
  - <sup>2</sup>See contributions in *Quantum Tunneling of Magnetization*, edited by L. Gunther and B. Barbara (Kluwer, Amsterdam, 1995).
  - <sup>3</sup>R. Sessoli, Hui-Lien Tsai, A. R. Shake, S. Wang, J. B. Vincent, K. Folting, D. Gatteschi, G. Christou, and D. N. Hendrickson, *J. Am. Chem. Soc.* **115**, 1804 (1993).
  - <sup>4</sup>L. Thomas *et al.*, *Nature (London)* **383**, 145 (1996); F. Lioni *et al.*, *J. Appl. Phys.* **81**, 4608 (1997); J. R. Friedman, M. P. Sarachik, J. Tejada, and R. Ziolo, *Phys. Rev. Lett.* **76**, 3830 (1996).
  - <sup>5</sup>W. Wernsdorfer and R. Sessoli, *Science* **284**, 133 (1999).
  - <sup>6</sup>M. N. Leuenberger and D. Loss, *Nature (London)* **410**, 789 (2001); F. Meier, J. Levy, and D. Loss, *Phys. Rev. B* **68**, 134417 (2003).
  - <sup>7</sup>C. Sangregorio, T. Ohm, C. Paulsen, R. Sessoli, and D. Gatteschi, *Phys. Rev. Lett.* **78**, 4645 (1997).
  - <sup>8</sup>A.-L. Barra, D. Gatteschi, L. Pardi, A. Müller, and J. Döring, *J. Am. Chem. Soc.* **114**, 8509 (1992).
  - <sup>9</sup>I. Chiorescu, W. Wernsdorfer, A. Müller, H. Bögge, and B. Barbara, *Phys. Rev. Lett.* **84**, 3454 (2000); *J. Magn. Magn. Mater.* **221**, 103 (2000); I. Chiorescu, W. Wernsdorfer, A. Müller, S. Miyashita, and B. Barbara, *Phys. Rev. B* **67**, 020402(R) (2003).
  - <sup>10</sup>G. Chaboussant, R. Basler, A. Sieber, S. T. Ochsenbein, A. Desmedt, R. E. Lechner, M. T. F. Telling, P. Kögerler, A. Müller, and H.-U. Güdel, *Europhys. Lett.* **59**, 291 (2002).
  - <sup>11</sup>S. Vongtragoon, B. Gorshunov, A. A. Mukhin, J. Slageren, M. Dressel, and A. Müller, *Phys. Chem. Chem. Phys.* **5**, 2778 (2003).
  - <sup>12</sup>H. De Raedt, S. Miyashita, and K. Michielsen, *Phys. Status Solidi B* **241**, 1180 (2004).
  - <sup>13</sup>G. Chaboussant, S. T. Ochsenbein, A. Sieber, H.-U. Güdel, H. Mutka, A. Müller, and B. Barbara, *Europhys. Lett.* **66**, 423 (2004).
  - <sup>14</sup>W. Wernsdorfer, A. Müller, D. Mailly, and B. Barbara, *Europhys. Lett.* **66**, 861 (2004).
  - <sup>15</sup>Y. Furukawa, Y. Fujiyoshi, K. Kumagai, and P. Kogerler, *Polyhedron* **24**, 2737 (2005).
  - <sup>16</sup>D. Proccisi, B. J. Suh, J. K. Jung, P. Kögerler, R. Vincent, and F. Borsa, *J. Appl. Phys.* **93**, 7810 (2003).
  - <sup>17</sup>A. Lascialfari, D. Gatteschi, F. Borsa, and A. Cornia, *Phys. Rev. B* **55**, 14341 (1997).
  - <sup>18</sup>Y. Furukawa, K. Kumagai, A. Lascialfari, S. Aldrovandi, F. Borsa, R. Sessoli, and D. Gatteschi, *Phys. Rev. B* **64**, 094439 (2001).
  - <sup>19</sup>M.-H. Julien, Z. H. Jang, A. Lascialfari, F. Borsa, M. Horvatic, A. Caneschi, and D. Gatteschi, *Phys. Rev. Lett.* **83**, 227 (1999).
  - <sup>20</sup>T. Moriya, *Prog. Theor. Phys.* **16**, 23 (1956).
  - <sup>21</sup>F. Borsa and A. Rigamonti, in *Magnetic Resonance at Phase Transitions*, edited by F. J. Owens, H. A. Farach, and C. P. Poole (Academic Press, New York, 1986).
  - <sup>22</sup>M. Luban, F. Borsa, S. Bud'ko, P. Canfield, S. Jun, J. K. Jung, P. Kögerler, D. Mentrup, A. Müller, R. Modler, D. Proccisi, B. J. Suh, and M. Torikachvili, *Phys. Rev. B* **66**, 054407 (2002).
  - <sup>23</sup>S.-H. Baek, M. Luban, A. Lascialfari, E. Micotti, Y. Furukawa, F. Borsa, J. van Slageren, and A. Cornia, *Phys. Rev. B* **70**, 134434 (2004).
  - <sup>24</sup>P. Santini, S. Carretta, E. Liviotti, G. Amoretti, P. Carretta, M. Filibian, A. Lascialfari, and E. Micotti, *Phys. Rev. Lett.* **94**, 077203 (2005).
  - <sup>25</sup>M. Corti, M. Filibian, P. Carretta, L. Zhao, and L. K. Thompson, *Phys. Rev. B* **72**, 064402 (2005).
  - <sup>26</sup>M. Belesi, A. Lascialfari, D. Proccisi, Z. H. Jang, and F. Borsa, *Phys. Rev. B* **72**, 014440 (2005).
  - <sup>27</sup>T. Goto, T. Koshihara, T. Kubo, and K. Agawa, *Phys. Rev. B* **67**, 104408 (2003).
  - <sup>28</sup>S.-H. Baek, Ph.D. thesis, Iowa State University, 2004.
  - <sup>29</sup>T. Kohmoto, T. Goto, S. Maegawa, N. Fujiwara, Y. Fukuda, M. Kunitomo, and M. Mekata, *Phys. Rev. B* **49**, 6028 (1994).